Fast computation of Hankel Transform using orthonormal exponential approximation of complex kernel function

Pravin K Gupta[1], Sri Niwas[1] and Neeta Chaudhary[2]

[1]Department of Earth Sciences, Indian Institute of Technology Roorkee, Roorkee 247 667, India.
[2]Oil and Natural Gas Corporation, Priyadarshini Building, Sion, Mumbai, India.

The computation of electromagnetic (EM) fields, for 1-D layered earth model, requires evaluation of Hankel Transform (HT) of the EM kernel function. The digital filtering is the most widely used technique to evaluate HT integrals. However, it has some obvious shortcomings. We present an alternative scheme, based on an orthonormal exponential approximation of the kernel function, for evaluating HT integrals. This approximation of the kernel function was chosen because the analytical solution of HT of an exponential function is readily available in literature. This expansion reduces the integral to a simple algebraic sum. The implementation of such a scheme requires that the weights and the exponents of the exponential function be estimated. The exponents were estimated through a guided search algorithm while the weights were obtained using Marquardt matrix inversion method. The algorithm was tested on analytical HT pairs available in literature. The results are compared with those obtained using the digital filtering technique with Anderson filters. The field curves for four types (A-, K-, H- and Q-type) of 3-layer earth models are generated using the present scheme and compared with the corresponding curves obtained using the Anderson scheme. It is concluded that the present scheme is more accurate than the Anderson scheme.

1. Introduction

Electromagnetic (EM) depth sounding is, under favourable conditions, extremely useful in petroleum exploration, groundwater exploration, permafrost thickness determination exploration of geothermal resources, and foundation engineering problems. However, for data interpretation one needs fast and efficient computations of geoelectromagnetic anomaly equations. These equations appear as Hankel Transform (HT) (also known as Bessel Transform) integral of the form:

$$E(r) = \int\limits_0^\infty G(\lambda) J_\nu(\lambda r) d\lambda. \qquad (1)$$

Here $J_\nu(\lambda r)$ is a Bessel function of real order ν of the first kind and it exhibits decaying, oscillatory behaviour for increasing argument along the real axis, r is usually the horizontal spacing, $G(\lambda)$ is referred to as kernel function as it appears under the integral sign. For most physical problems, the order of the Bessel function is an integer, and only 0 and 1 need to be considered. The higher order Bessel functions are related to these by standard recursion formulae. Integrals of the form (1) can be evaluated in closed form only for a restricted set of kernel functions (Watson 1962) and a recourse to numerical methods is necessary for the study of real problems (Chave 1983). The oscillatory nature of J_ν and the infinite range of the integral renders its numerical evaluation difficult. For details of the currently used techniques for numerical evaluation of this integral, one can refer to Frischknecht (1967); Anderson (1979, 1982); Kaufman and Keller (1983); Nabighian (1988).

The popular approach to the computation of HT is the application of digital linear filter method initially suggested by Kunetz (1966) and developed
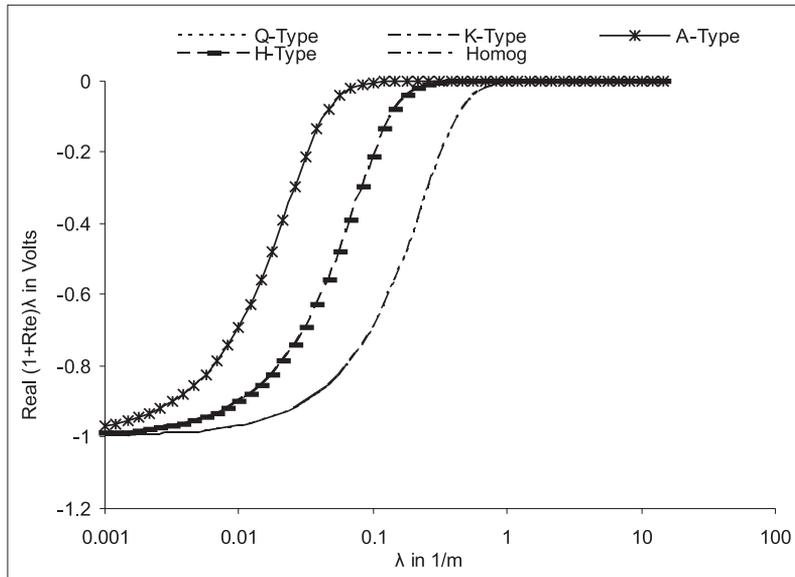
Figure 1. Plots of real part of EM resistivity transform showing their similarity to the dc resistivity transform curve.

by Ghosh (1971a, b) for real kernel functions. The linear filter approach was extended for a complex kernel by Koefoed *et al* (1972). The pre-linear filter attempts of computations may be found in Wait (1955, 1958), Keller and Frischknecht (1966), Frischknecht (1967), Vanyan (1967). In the filter approach suitable changes of the independent variables r and λ in equation (1) transforms the direct integrals into a convolution integral. The Bessel function of the new variable plays the role of a filter through which the kernel function is passed as the signal to get the transformed result as the filter output. Since the work of Koefoed *et al* (1972), significant improvements have been made by various workers in the design of filters. The filter design criteria are primarily *ad hoc* and are discussed by Anderson (1979) while introducing his set of digital filters. He claimed reasonable accuracy by considering monotonic, rapidly decreasing kernel functions at moderate values of r. The key to successful numerical evaluation of equation (1) lies in defining appropriate filter weights that can be used for a wide variety of input–output pairs. Anderson (1979) has taken 283 filter weights, which increase the efficiency of computation in comparison to old numerical methods. Further development by Anderson (1982) was to include adaptive and lagged convolution to minimize kernel function evaluations. An alternative approach for computing optimal filter coefficients was proposed by Johansen and Sorensen (1979) and by Christensen (1990). This approach even provides *a priori* error estimates of filters. However, it has been noticed that for some types of problems the digital filter method is less useful, examples occur at very small values of the range r, where the kernel functions

may be changing rapidly when compared to the Bessel function, and when high numerical precision is required (Chave 1983).

Sri Niwas and Israil (1986) noticed similar shortcomings while using Ghosh (1971a, b) filters. They presented an alternative efficient approach for computation of HT in dc resistivity methods by approximating HT kernel as a superposition of exponential terms. This reduces the integral to a simple algebraic sum. They used 12 coefficients of approximation, which is very small in comparison to Anderson's 283 filter weights. Thus the computations required are extensively reduced. Success of this approach in dc, motivated us to extend this scheme further to EM problems. This view was further supported by the similarity in behaviour of the dc kernel and resistivity curves to the real and imaginary components of EM kernel of layered half space and the field of homogeneous half space.

To implement the scheme, we started with some analytical HT pairs. Five such integrals were also used by Anderson (1979). We also implemented our scheme on the EM field of Vertical Magnetic Dipole (VMD) over a homogeneous half space model, its analytical solution is available in literature and for an exhaustive study of this scheme we used a constant function (unity) as integrand of approximation. In total we used eight analytical integral pairs.

2. Behaviour of EM kernel and field

The EM kernel and field behaviours for various layered half-space models were used to study the kernel function curves. For example, the real and imaginary part of kernel curves for
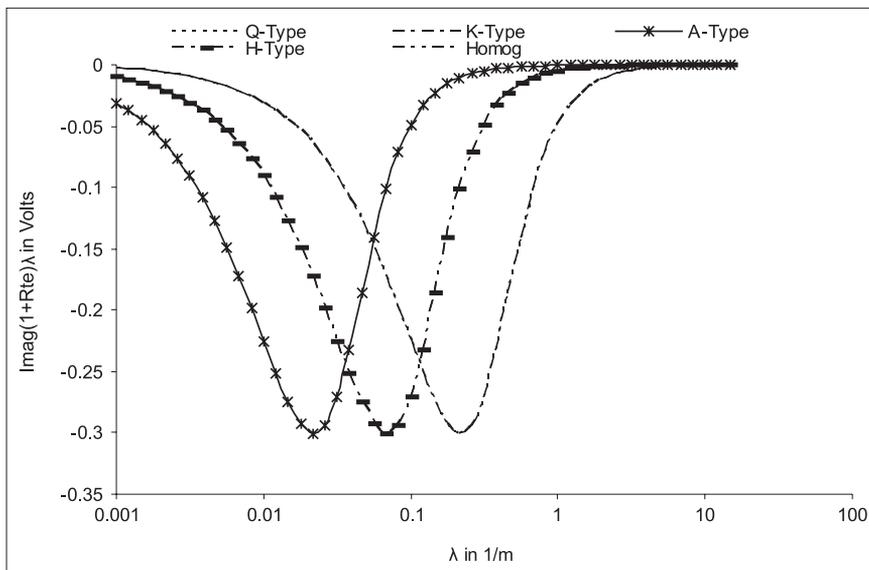
Figure 2. Plots of imaginary part of EM resistivity transform showing their similarity to dc resistivity transform.

3-layer sequences of A-type ($\sigma_1 > \sigma_2 > \sigma_3$), K-type ($\sigma_1 > \sigma_2 < \sigma_3$), H-type ($\sigma_1 < \sigma_2 > \sigma_3$), and Q-type ($\sigma_1 < \sigma_2 < \sigma_3$) earth models are computed for real and imaginary parts of the field due to a VMD source on a homogeneous half-space model. If we compare these results with the corresponding direct current (dc) source results, it is evident that variation of the real part of the EM kernel shows the same behaviour as the A-type curves of the dc kernels (figure 1) while the curves of the imaginary part of the EM kernel shows the same behaviour as the H-type curves of the dc kernels (figure 2). The variation of the imaginary part of the EM field due to a VMD source on a homogeneous half-space model, shows similarity with the dc resistivity curves (figures 1–2). After establishing that the variation of the EM kernel and field is similar to the dc kernel and resistivity curves, we took up the task of developing the scheme for EM computations.

The scheme has been applied to the computation of electric field component due to a VMD source over a layered earth. The fields, having time dependence $e^{i\omega t}$, are obtained by solving the following equation for vector potential A,

$$\nabla^2 \boldsymbol{A} + k^2 \boldsymbol{A} = \boldsymbol{S}. \tag{2}$$

$\boldsymbol{S}$ is the source term, and k is the wave number. However, for a VMD source over a layered earth, the vector potential $\boldsymbol{A}$ has only one non-zero component A_z and thus equation (2) becomes a scalar potential equation. For a VMD source over a layered earth only E_ϕ component of the field is non-zero. Hence, from now onwards only E_ϕ component of the field will be used as electric field. The electric field at height z for a VMD of moment, m, situated at height h over a layered half space, is given by

$$E_\phi(r) = \frac{-\hat{z}_0 m}{4\pi} \int\limits_0^\infty \left[e^{-u_0(z+h)} + R_{te} e^{u_0(z-h)} \right]$$

$$\times \frac{\lambda^2}{u_0} J_1(\lambda r) d\lambda. \tag{3}$$

Here, R_{te}, the reflection function of layered earth, is given as (Ward and Hohmann 1988),

$$R_{te} = \frac{Y_0 - \hat{Y}_1}{Y_0 + \hat{Y}_1}, \tag{4}$$

with

$$Y_0 = \frac{u_0}{\hat{z}_0} \quad \text{(intrinsic admittance of free space)}. \tag{5}$$

For an N-layer model $\hat{Y}_1$, the surface admittance of the first layer, is given as

$$\hat{Y}_1 = Y_1 \frac{\hat{Y}_2 + Y_1 \tanh(u_1 d_1)}{Y_1 + \hat{Y}_2 \tanh(u_1 d_1)}. \tag{6}$$

For an arbitrary layer $n(1 < n < N)$ the interface admittance will be

$$\hat{Y}_n = Y_n \frac{\hat{Y}_{n+1} + Y_n \tanh(u_n d_n)}{Y_n + \hat{Y}_{n+1} \tanh(u_n d_n)}. \tag{7}$$

Finally, for the half-space, the admittance is given as

$$\hat{Y}_N = Y_N.$$

Here,

$$Y_n = \frac{u_n}{\hat{z}_n},$$

$$u_n = \sqrt{(\lambda^2 - k_n^2)},$$

$$\lambda^2 = k_x^2 + k_y^2,$$

$$k_n^2 = \omega^2 \mu_n \varepsilon_n - i\omega\mu_n\sigma_n \approx -i\omega\mu_n\sigma_n,$$

$$\omega = 2\pi f,$$

$$\hat{z}_0 = i\omega\mu_0,$$

$$\hat{z}_n = i\omega\mu_n$$

and f is frequency of the source field while μ_n, ε_n, σ_n and d_n are magnetic permeability, electric permitivity, conductivity and thickness of the nth layer. It may be added here that magnetic permeability for all layers is assumed to be μ_0, the permeability of vacuum. Further, z is depth up to top of the layer, λ is integral parameter, r is spacing between source and receiver.

$\hat{Y}_1$ is determined recursively by starting at the deepest layer and iterating upwards. For calculations, it may be desirable to formulate the *tanh* term in terms of negative exponentials for greater numerical stability.

If the source and the receiver are on the surface of the earth, then h and z are set to zero and u_0 becomes λ. Now equation (3) reduces to

$$E_\phi(r) = \frac{-\hat{z}_0 m}{4\pi} \int_0^\infty (1 + R_{te})\lambda J_1(\lambda r) d\lambda. \qquad (8)$$

For homogeneous half space the field integral is analytical and its solution is given as

$$E_\phi(r) = \frac{-m}{2\pi\sigma r^4} \left[3 - (3 + 3ikr - k^2r^2)e^{-ikr}\right]. \qquad (9)$$

For details of derivation of the above equations one can refer to Nabighian (1988). The behaviours of the EM kernel and field were studied before implementation of the scheme.

3. Exponential approximation scheme (EAS)

The kernel in equation (1) when approximated as a superposition of exponential terms, enables evaluation of the integral in an analytical form. So, let the kernel be approximated as

$$G(\lambda_j) = \sum_{i=1}^N a_i e^{-\varepsilon_i \lambda_j}. \qquad (10)$$

Here, a_is are the coefficients of superposition and ε_is are parameters of approximation. For the set of M different λ values, the equation (10) can be written in matrix form as

$$\boldsymbol{G} = \boldsymbol{M}\boldsymbol{a}. \qquad (11)$$

Here $\boldsymbol{a}$ is the column vector of coefficients of approximation for the N ε-values and $\boldsymbol{G}$ is the column vector of kernel values for the M λ-values. The elements of the $M \times N$ matrix $\boldsymbol{M}$ are given as,

$$M_{ji} = e^{-\varepsilon_i \lambda_j}.$$

When this approximated kernel is substituted in the integral, the field is transformed as,

$$E_\phi(r) = \sum_{i=1}^N a_i \int_0^\infty e^{-\varepsilon_i \lambda} J_\nu(\lambda r) d\lambda. \qquad (12)$$

This integral can be evaluated using the Lipschitz integral,

$$\int_0^\infty e^{-\varepsilon\lambda} J_\nu(\lambda r) d\lambda = \frac{1}{\sqrt{\varepsilon^2 + r^2}} \left[\frac{r}{\sqrt{\varepsilon^2 + r^2} + \varepsilon}\right]^\nu. \qquad (13)$$

If $\nu = 1$ then,

$$\int_0^\infty e^{-\varepsilon\lambda} J_1(\lambda r) d\lambda = \frac{1}{\sqrt{\varepsilon^2 + r^2}} \frac{r}{\sqrt{\varepsilon^2 + r^2} + \varepsilon}. \qquad (14)$$

Now equation (12) can be written as

$$E_\phi(r) = \sum_{i=1}^N a_i \frac{1}{\sqrt{\varepsilon_i^2 + r^2}} \frac{r}{\sqrt{\varepsilon_i^2 + r^2} + \varepsilon_i}. \qquad (15)$$

For the set of P different values of r, this equation can be written in matrix form,

$$\boldsymbol{E} = \boldsymbol{N}\boldsymbol{a}, \qquad (16)$$

where, $\boldsymbol{E}$ is the column vector of the field values for the P r-values and the elements of the $P \times N$ matrix $\boldsymbol{N}$ are given as,

$$N_{ji} = \frac{1}{\sqrt{\varepsilon_i^2 + r_j^2}} \frac{r_j}{\sqrt{\varepsilon_i^2 + r_j^2} + \varepsilon_i}.$$

The exponential scheme can be used for solving either the forward (computation of field values from given kernel values) or the inverse (computation of kernel values from given field values) problem. For the forward or the inverse case the coefficient vector $\boldsymbol{a}$ is evaluated through Marquardt inversion of equation (11) or (16). This vector is then used either in equation (16) or in

equation (11) to compute either the field vector $\boldsymbol{E}$ or the kernel vector $\boldsymbol{G}$. In the half-space case, the approximated field values are compared with the true analytical field values obtained using equation (9). The absolute and relative root mean square (RMS) errors are estimated using the following formulae:

$$\text{Abs error}_i = \text{abs}(\text{True value}_i - \text{Approx. value}_i),$$
(17)

$$\text{Rel error}_i = \frac{\text{abs error}_i}{\text{True value}_i},$$
(18)

$$\text{Absolute RMS error} = \sqrt{\sum_{i=1}^{M} \frac{(\text{abs error}_i)^2}{M}}, \quad (19)$$

$$\text{Relative RMS error} = \sqrt{\sum_{i=1}^{M} \frac{(\text{Rel error}_i)^2}{M}}. \quad (20)$$

4. Development of EAS-software

In order to define the exponential terms in the interpolant and the matrix elements, the ε_i's should be known *a priori*. These values were estimated through a guided search subjected to minimum RMS error. For the search of ε values, we have chosen the 5 analytical integrals given by Anderson (1979) along with the two integrals of real and imaginary parts of EM fields due to a VMD on a homogeneous half-space model. For an exhaustive study the integral for unity, an extreme case, was also included. These eight analytical integral pairs are given below:

$$\int_0^{\infty} \lambda \exp(-\lambda^2) J_0(\lambda r) \, d\lambda = \frac{1}{2} \exp\left(\frac{-r^2}{4}\right),$$
Integral 1 (21)

$$\int_0^{\infty} \lambda^2 \exp\left(-\lambda^2\right) J_1(\lambda r) \, d\lambda = \frac{r}{4} \exp\left(\frac{-r^2}{4}\right),$$
Integral 2 (22)

$$\int_0^{\infty} \exp(-\lambda) J_1(\lambda r) \, d\lambda = \frac{\sqrt{1+r^2}-1}{r\sqrt{1+r^2}},$$
Integral 3 (23)

$$\int_0^{\infty} \lambda \exp(-2\lambda) J_1(\lambda r) \, d\lambda = \frac{r}{(4+r^2)^{3/2}},$$
Integral 4 (24)

$$\int_0^{\infty} \exp(-2\lambda) J_0(\lambda r) \, d\lambda = \frac{1}{\sqrt{4+r^2}},$$
Integral 5 (25)

$$E_{\phi}(r) = -\frac{\hat{z}_0 m}{4\pi} \int_0^{\infty} (1 + R_{te}) \lambda J_1(\lambda r) \, d\lambda$$

$$= \left(-\frac{m}{2\pi\sigma r^4}\right) \left[3 - \left(3 + 3ikr - k^2 r^2\right) e^{-ikr}\right]$$
Integrals 6 (real) and 7 (imaginary) (26–27)

and

$$\int_0^{\infty} \lambda \, J_1(\lambda r) \, d\lambda = \frac{1}{r^2}. \qquad \text{Integral 8} \quad (28)$$

4.1 *Search for epsilon*

We started with the Geometric Progression (GP) range of ε, used by Sri Niwas and Israil (1986) for the dc resistivity case. The GP set used was 0.2 (2.0) 409.6, where 0.2 is the first value, 2.0 is the common ratio and 409.6 is the last 12th point in the series. With this range of values none of the integrals could be matched with the corresponding analytical value. We gradually increased the number of ε values from 12 to 51 and reduced the common ratio from 2 to 1.2. The initial value taken was 0.5. We fixed the range of λ-values taken in log-series in the practical range. The first value was 0.001, number of points per decade was 12, the last value was 14.678 and the total number of points was 51.

After experimenting with different sets of ε values, we found that with the GP set of 51 values in the range 0.5 (1.2) 4550.2, the third (equation 23), fourth (equation 24) and fifth (equation 25) integrals were matched with the corresponding analytical values while all the other integrals were not. To reproduce the Anderson results, the integrals were evaluated at the same r values as used by Anderson (1979).

To compare the results of the VMD field the practical range of r values were taken in log series. The first value was 1.0, number of points per decade was 10, the last value was 1000 and the total number of points used was 31.

Table 1. *Relative error for the first five integrals using EAS.*

r	Integral 1	Integral 2	Integral 3	Integral 4	Integral 5
$1.00E-04$	$6.38E-06$	$4.39E-04$	$3.71E-08$	$5.39E-08$	$2.76E-10$
$1.00E-03$	$6.38E-06$	$4.39E-04$	$4.08E-08$	$5.39E-08$	$2.76E-10$
$5.00E-03$	$6.37E-06$	$4.39E-04$	$4.06E-08$	$5.38E-08$	$2.75E-10$
$1.00E-02$	$6.33E-06$	$4.37E-04$	$4.04E-08$	$5.36E-08$	$2.73E-10$
$5.00E-02$	$5.14E-06$	$3.80E-04$	$3.50E-08$	$4.65E-08$	$2.05E-10$
$1.00E-01$	$2.42E-06$	$2.37E-04$	$2.14E-08$	$2.88E-08$	$5.06E-11$
$5.00E-01$	$1.09E-06$	$5.11E-06$	$3.30E-10$	$5.51E-10$	$2.79E-11$
$1.00E+00$	$1.79E-06$	$1.39E-06$	$1.14E-10$	$1.57E-10$	$6.50E-12$
$2.00E+00$	$3.80E-06$	$7.36E-07$	$2.71E-11$	$5.39E-11$	$7.16E-12$

Table 2. *Relative error for the first five integrals using the Anderson scheme.*

r	Integral 1	Integral 2	Integral 3	Integral 4	Integral 5
$1.00E-04$	$1.07E-06$	$2.18E-07$	$3.64E-07$	$1.46E-07$	$2.81E-05$
$1.00E-03$	$4.77E-07$	$0.00E+00$	$3.64E-07$	$0.00E+00$	$2.62E-06$
$5.00E-03$	$1.07E-07$	$2.79E-07$	$3.64E-07$	$4.66E-07$	$5.96E-07$
$1.00E-02$	$1.10E-07$	$1.86E-07$	$3.64E-07$	$9.31E-08$	$7.15E-07$
$5.00E-02$	$1.19E-07$	$2.24E-07$	$3.64E-07$	$0.00E+00$	$2.38E-07$
$1.00E-01$	$1.20E-07$	$1.49E-07$	$3.64E-07$	$7.48E-08$	$1.19E-07$
$5.00E-01$	$1.27E-07$	$1.27E-07$	$3.64E-07$	$5.88E-07$	$0.00E+00$
$1.00E+00$	$3.83E-07$	$2.45E-06$	$3.64E-07$	$1.67E-07$	$2.67E-07$
$2.00E+00$	$1.86E-06$	$5.91E-06$	$3.64E-07$	$8.43E-07$	$8.43E-08$

4.2 *Gram Schmidt's orthonormalization*

While looking for possible causes for the mismatch of remaining integrals, we discovered that the matrix, $\boldsymbol{M}$, was highly unstable with its determinant value being of the order of 10^{-280}. To overcome this problem, we employed the Gram Schmidt's Orthonormalization (GSO) of the exponential functions. For implementation of GSO scheme one can refer Press *et al* (1993). Application of GSO enhanced the determinant value to 10^{-28}. The results were improved significantly. All the five integrals of Anderson were now matched. However, the other three integrals were still not matching.

4.3 *Use of mutual coupling ratio*

When we further searched for possible causes of error, it was discovered that the geometrical spreading $(1/r^2)$ factor in equation (27) was making the field values to be very large at too low or too high r values. To remove this effect, we used the mutual coupling ratio defined as the ratio of the EM field in medium with the field in vacuum. The field in vacuum is only generated by the source and is referred to as the primary field and is given by

$$E_\phi^{(0)} = \frac{i\omega\mu_0 m}{4\pi r^2}. \tag{29}$$

When the electric field component given in equation (27) was normalized with the primary field

given by equation (29), the geometrical spreading effect was removed. The normalized field $e_\phi(r)$ is given as

$$e_\phi(r) = -r^2 \int\limits_0^\infty \left[e^{u_0(z+h)} + R_{te}e^{u_0(z-h)} \right]$$
$$\times \frac{\lambda^2}{u_0} J_1(\lambda r)d\lambda. \tag{30}$$

For a homogeneous half space the normalized analytical field is now given as

$$e_\phi(r) = \frac{2}{k^2 r^2} \left[3 - \left(3 + 3ikr - k^2 r^2 \right) e^{-ikr} \right]. \tag{31}$$

Here $k^2 = -i\omega\mu_0\sigma$.

On applying the EAS scheme on the normalized electric fields, the imaginary part of the field was matched but the real part of the field and the integral for unity were still not matching.

4.4 *Choice of integrand*

From a study of the integral of unity, equation (28), we found that the λ term as integrand was resulting in poor approximation. To avoid this numerical problem, we removed the λ term from the integrand and merged it with the Bessel function. Thus a new analytical solution, given below, was used
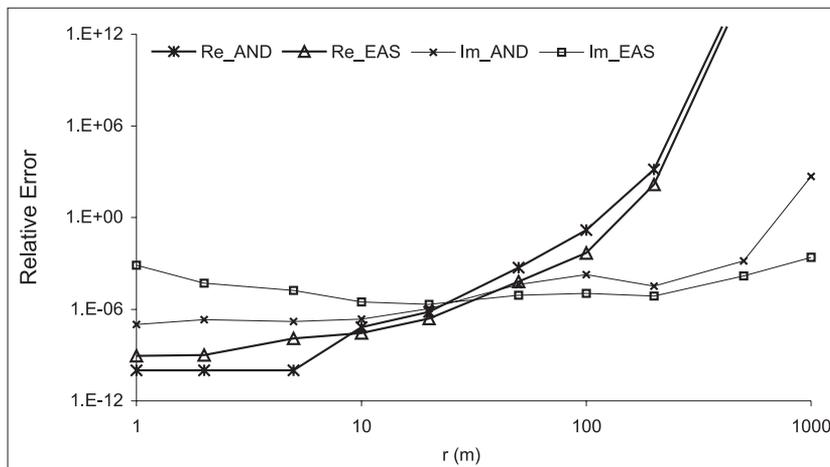
Figure 3. The relative errors in the real and imaginary components of the electric field of a half space due to a VMD source using the Anderson scheme (Re_AND and Im_AND) and the EAS (Re_EAS and Im_EAS).
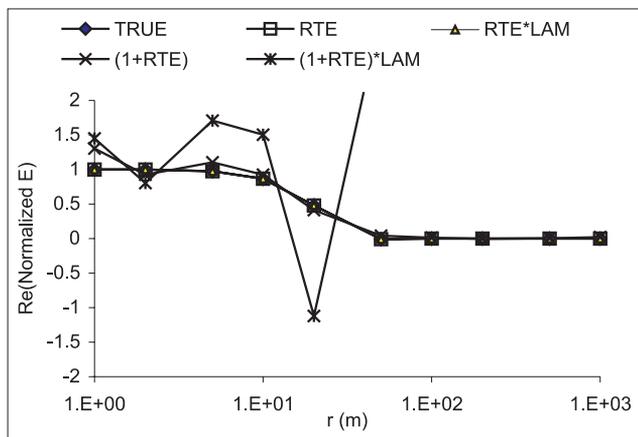

Figure 4. The real component of the normalized electric field of a half space due to a VMD source using different integrands in the EAS. RTE is R_{TE} and LAM is λ.
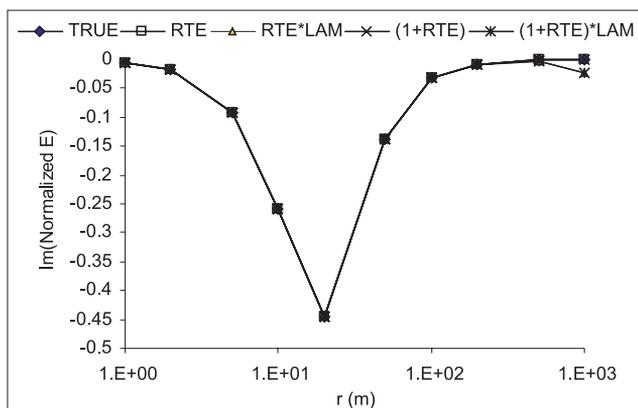

Figure 5. The imaginary component of the normalized electric field of a half space due to a VMD source using different integrands in the EAS. RTE is R_{TE} and LAM is λ.

for the integral

$$\int_0^\infty e^{-\lambda\varepsilon}\lambda\,J_1\left(\lambda r\right)\,d\lambda = \frac{r}{\left(r^2+\varepsilon^2\right)^{3/2}}. \qquad (32)$$
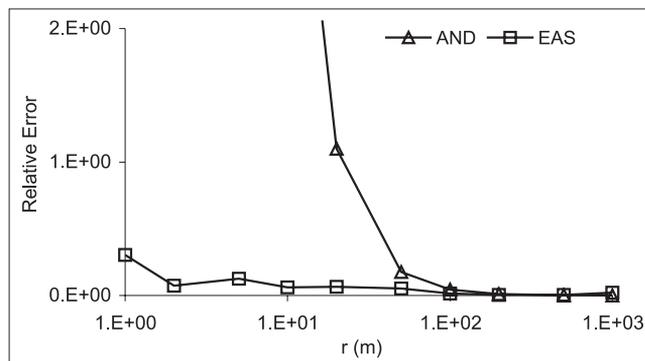

Figure 6. The relative errors in the computation of unity integral using the Anderson scheme (AND) and the EAS (EAS).

This change in the integrand function significantly improved the results of the integral for unity. Taking cue from this, we applied the same changes in the kernel of the field integral letting only R_{te} constitute the integrand and incorporating the λ term with the Bessel function. The integral for unity term is separately evaluated analytically and added. Now the real part of the field was also matched.

5. Evaluation of EAS

5.1 *Integrals used by Anderson (1979)*

We compared the results given by Anderson (1979) for the five analytical integrals with the corresponding EAS computed results. The relative errors for these five integrals for the two schemes are given in tables 1–2.

From these two tables it is evident that the two schemes yield values of the same order for the first two integrals while for the last three integrals EAS
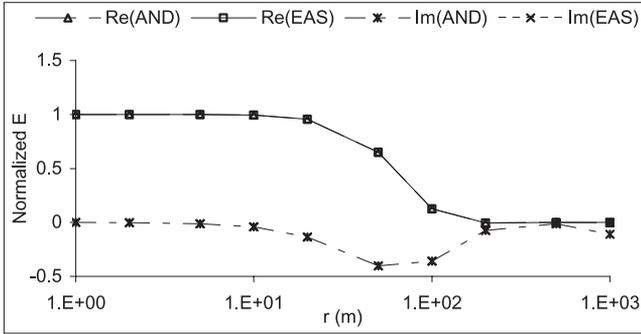
Figure 7. The real and imaginary normalized electric field curves of A-type 3-layer model computed using the Anderson scheme (Re–AND and Im–AND) and the EAS (Re–EAS and Im–EAS).
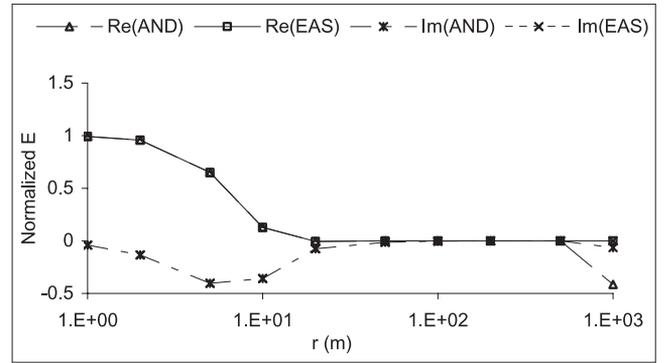

Figure 9. The real and imaginary normalized electric field curves of Q-type 3-layer model computed using the Anderson scheme (Re–AND and Im–AND) and the EAS (Re–EAS and Im–EAS).
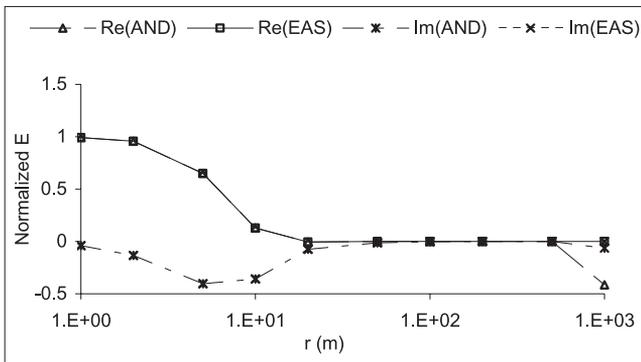

Figure 8. The real and imaginary normalized electric field curves of K-type 3-layer model computed using the Anderson scheme (Re–AND and Im–AND) and the EAS (Re–EAS and Im–EAS).
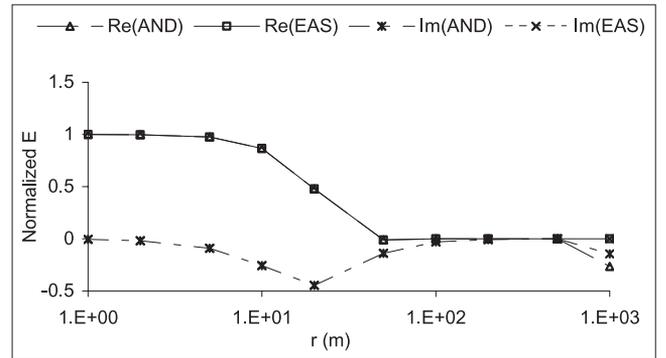

Figure 10. The real and imaginary normalized electric field curves of H-type 3-layer model computed using the Anderson scheme (Re–AND and Im–AND) and the EAS (Re–EAS and Im–EAS).

yields better results than those from the Anderson scheme.

5.2 *Electric field e_ϕ for a homogeneous half space*

The EAS and Anderson schemes were also compared for the EM field of a homogeneous half space of 1 Ohm m resistivity due to a VMD source of frequency 250 Hz. The relative errors in the two cases for both real and imaginary components are given in figure 3. It is evident from this figure that the EAS results are comparable with the Anderson results for the low (<10 m) r values while the former is better for the larger (>10 m) r values.

5.3 *Choice of integrand*

The relative errors for the real and imaginary parts of the e_φ field using different integrand functions for approximation in the EAS are given in figures 4 and 5. From these figures it is clear that the integrand function R_{te} yields the best results.

5.4 *Extreme case – unity integral*

EAS was also compared with the Anderson scheme for the analytical unity integral. In this case the integrand is unity and hence it amounts to integral of Bessel function only. The approximation of a constant function (unity) is always susceptible to large oscillations if the scheme is not stable. The relative errors for this integral using the two schemes are given in figure 6. It is evident that the EAS results are far better than the Anderson scheme results.

5.5 *3-layer models*

To further check the stability of EAS scheme, we generated and compared the results for different 3-layered half-space models of A, K, H and Q type. The frequency of VMD source was taken as 250 Hz. The model parameters used are given below:
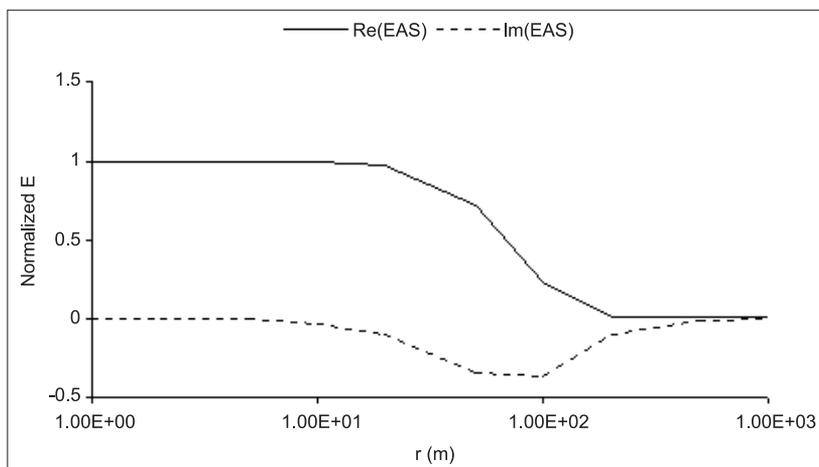
Figure 11. The real and imaginary normalized electric field curves of 3-layer high resistivity contrast model (1,100,1 Ohm m), computed using the EAS (Re$_-$EAS and Im$_-$EAS).

Layer	Thickness	A-type Res	H-type Res	K-type Res	Q-type Res
	(m)	(Ω-m)	(Ω-m)	(Ω-m)	(Ω-m)
1	5.0	0.01	0.1	0.01	1.0
2	5.0	0.1	0.01	0.1	0.1
3	Half space	1.0	0.1	0.01	0.01

The real and imaginary components evaluated using the two schemes are given in figures 7–10 for the A, Q, K and H-type models respectively. The imaginary component of the field evaluated using the Anderson scheme for the three-layer models tend to deviate significantly from the true value at large values of r, while the EAS gives smooth curves in the entire range of r values.

In order to see the impact of high resistivity contrast on the stability of EAS scheme, the response of a 3-layer model with resistivities 1, 100 and 1 Ohm m was computed and is presented in figure 11. It is clear that the pattern is still well behaved.

6. Conclusions

The exponential approximation of the EM kernel leads to an efficient scheme of HT computation. The Gram Schmidt's orthogonalization of exponential functions significantly improves the stability of the coefficient matrix. The use of mutual coupling ratio data further improves the versatility of EAS. The stability of the EAS scheme in case of high resistivity contrast models is illustrated by the well-behaved nature of the responses.

Out of the several possible ways of choosing the integrand in the field integral (30), the choice of R_{te} as integrand yields the best results.

Finally, it may be emphasized that the EAS coefficient matrix when inverted and stored for a given set of r values needs a simple matrix multiplication step to transform field to kernel and *vice versa*. Such a multiplication will require only 51 multiplications for the present set up in comparison to the 283 point convolution in the Anderson scheme making the former more efficient.

References

Anderson W L 1979 Numerical integration of related HTs of orders 0 and 1 adaptive digital filtering; *Geophysics* **44** 1287–1305.

Anderson W L 1982 Fast HTs using related and lagged convolution; *ACM Trans. Math. Software* **8** 344–368.

Chave A D 1983 Numerical integration of related HTs by quadrature and continued fraction expansion; *Geophysics* **48** 1671–1686.

Christensen N B 1990 Optimized fast Hankel Transform filters; *Geophys. Prosp.* **38** 545–568.

Frischknecht F C 1967 Fields about an oscillating magnetic dipole over a two-layer earth, an application to ground and airborne electromagnetic surveys; *Quart. Colorado School of Mines* **62** 326.

Ghosh D P 1971a The application of linear filter theory to the direct interpretation of geoelectrical resistivity sounding measurements; *Geophys. Prosp.* **19** 192–217.

Ghosh D P 1971b Inverse filter coefficients for the computation of apparent resistivity standard curves for a horizontally stratified earth; *Geophys. Prosp.* **19** 769–775.

Johansen H K and Sorensen K 1979 Fast Hankel Transforms; *Geophys. Prosp.* **27** 876–901.

Kaufman A A and Keller G V 1983 Frequency and Transient Soundings (Netherlands: Elsevier).

Keller G V and Frischknecht F C 1966 Electrical methods in geophysical prospecting (Oxford: Pergamon).

Koefoed O, Ghosh D P and Polman G J 1972 Computation of type curves for electromagnetic depth sounding with a horizontal transmitting coil by means of a digital linear filter; *Geophys. Prosp.* **20** 406–420.

Kunetz G 1966 *Principles of direct current resistivity prospecting* (Gebruder-Borntraeger).

Nabighian M N 1988 *Electromagnetic methods in applied geophysics-Theory*; **1** (SEG publication).

Press W H, Teukolsky S A, Vellerling W T and Flannery B P 1993 *Numerical Recipes in Fortran* (Cambridge University Press, First Indian Edition).

Sri Niwas and Israil M 1986 Computation of apparent resistivities using an exponential approximation of kernel functions; *Geophysics* **51** 1594–1602.

Vanyan L L 1967 *Electromagnetic depth sounding* (New York: Consultants Bureau).

Wait J R 1955 Mutual electromagnetic coupling of loops over a homogeneous ground; *Geophysics* **20** 630–637.

Wait J R 1958 Induction by an oscillating magnetic dipole over a two-layer ground; *Appl. Sci. Res.* **7** 73–80.

Ward S H and Hohmann G W 1988 Electromagnetic theory for geophysical applications; In: *Electromagnetic methods in applied geophysics – Theory*; (ed.) Nabighian M N, SEG publication.

Watson G N 1962 *A treatise on the theory of Bessel functions* (Cambridge: Cambridge University Press).